The dual role of viscosity in capillary rise

Joachim Delannoy, Suzanne Lafont, Yukina Koga,
Étienne Reyssat & David Quéré

Physique & Mécanique des Milieux Hétérogènes, UMR 7636 du CNRS, ESPCI Paris,
PSL Research University, Sorbonne Université, Université Paris Diderot, 75005 Paris, France.

Supplementary Information

1. Derivation of the viscous friction in the meniscus

Here, we briefly recall the derivation by Moffatt of the pressure exerted by a viscous fluid moving in a corner, a situation sketched in figure SI1 [18].

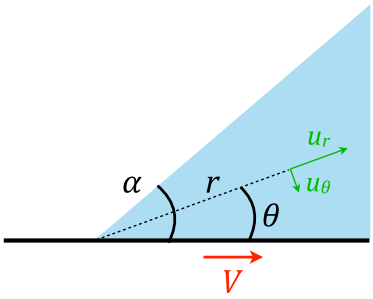

Figure SI1. Sketch of a liquid wedge (blue) with apparent angle α moving on a solid surface (black line) at a velocity V, in the reference frame of the wedge. u_r and u_θ are the fluid velocity in the coordinates (r, θ).

Denoting the wedge angle as α and its speed as V, the flow is described in the reference frame of the moving wedge by a stream function ψ, that verifies $u_r = 1/r(\partial\psi/\partial\theta)$, and $u_\theta = -\partial\psi/\partial r$, where u_r and u_θ are the radial and tangential velocities in coordinates (r, θ). For a viscous flow, ψ is a solution of the Stokes equation, $\nabla^4\psi = 0$, whose solutions can be decomposed as $\psi = V r^\lambda f(\theta)$. Close to the tip of the wedge, the solutions must verify $\lambda = 1$ to obtain a non-trivial, finite velocity for $r \to 0$. The boundary conditions are $u_r = V$ and $u_\theta = 0$ at the liquid-solid interface, and $u_\theta = 0$ and a shear stress $\sigma_{\theta r} = 0$ at the liquid-gas

interface, which implies $f'(0) = 1$, $f(0) = 0$, $f(\alpha) = 0$ and $f''(\alpha) - f(\alpha) = 0$. Solving the Stokes equation with these boundaries conditions for $\psi = V r f(\theta)$ yields:

$$\psi = rV\frac{\alpha\sin\theta - \theta\sin\alpha\cos(\theta - \alpha)}{\alpha - \sin\alpha\cos\alpha} \equiv rV.g_\alpha(\theta) \quad \text{(SI.1)}$$

where we introduced the function g_α for clarity. The pressure gradient obeys $\nabla p = \eta\Delta u$, and its projection along the radial coordinate is:

$$\frac{\partial p}{\partial r} = \eta\left(\frac{\partial^2 u_r}{\partial r^2} + \frac{1}{r^2}\frac{\partial^2 u_r}{\partial\theta^2} + \frac{1}{r}\frac{\partial u_r}{\partial r} - \frac{2}{r^2}\frac{\partial u_\theta}{\partial\theta} - \frac{u_r}{r^2}\right) = \frac{\eta V}{r^2}[g_\alpha^{(3)}(\theta) + g_\alpha'(\theta)] \quad \text{(SI.2)}$$

Integrating along r at the liquid-air boundary ($\theta = \alpha$) gives the pressure induced by the fluid motion on the moving interface:

$$p_f(\alpha) = -\frac{\eta V}{r}\left[g_\alpha^{(3)}(\alpha) + g_\alpha'(\alpha)\right] = \frac{2\eta V}{y}\frac{\sin^2\alpha}{\alpha - \sin\alpha\cos\alpha} \quad \text{(SI.3)}$$

where $y = r/\sin\alpha$ represents the local thickness of liquid as defined in figure 4b.

2. Prewetting the tubes

In order to prewet the tube walls, we place a slug of oil with centimetric length l and tilt the tube by an angle β with respect to the vertical. The slug reaches a steady state as its weight $\sim\rho r^2 lg\cos\beta$ is balanced by the viscous friction $\sim\eta lU$, where U is the slug velocity that can be controlled by the inclination of the tube (figure SI.2 (a)). For each experiment with prewet tubes, we measure the velocity U by timing the descent in tubes of known length. The thickness ε of the deposited film is then calculated using Bretherton's formula $\varepsilon = 1.34\, r(\eta U/\gamma)^{2/3}$ [13]. As seen in figure SI.2 (b), ε can also by deduced from the shortening Δl of the liquid slug along its descent. In this case, we measure $\varepsilon = r\,\Delta l/2U\Delta t = 21$ μm, in good agreement with the value expected using Bretherton's formula, that is, 22 μm. When the drop reaches the end of the tube, we

remove it gently by absorbing the oil with a paper, and then perform the experiment presented in figure 1 with the other side of the tube.

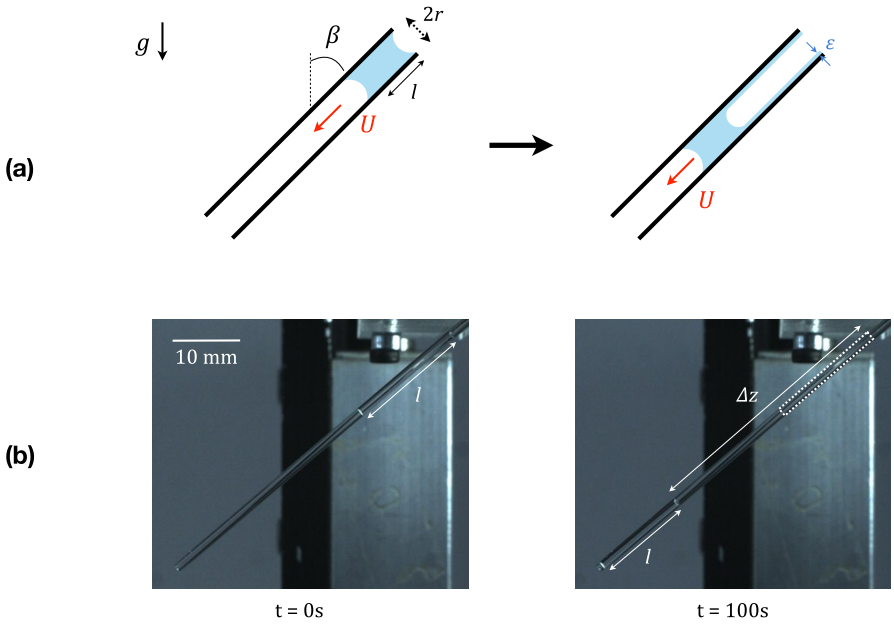

Figure SI2. (a) Sketch of an oil slug (in blue) of initial length l advancing at a constant speed U in a tube of radius r inclined by an angle β to the vertical. As it moves, the slug deposits a liquid film of thickness ε on the tube walls. **(b)** Pictures of a drop advancing in a tube with r = 0.5 mm and $\beta = 50°$. In the left picture, the drop length is l = 16.7 mm. In the right picture, that is, Δt =100s later, the drop has progressed by Δz = 37 mm, at velocity U = 0.37 mm/s, and its length has become l = 13.5 mm. The thickness of the deposited film deduced from the slug shortening is 21 μm.

3. Meniscus shape and macroscopic contact angle

Eq. 3 is an implicit equation between h and $\theta = \mathrm{d}h/\mathrm{d}x$ that we can integrate using a numerical solver (such as ode15i with MATLAB). The shape of the meniscus depends on its velocity, whose initial value is given by eq. 4: $V \approx \gamma\pi^3 / (72 \ln r/\varepsilon)$. Later, the meniscus speed $\dot{z}$ decreases during the rise because of bulk viscous dissipation and gravity. We sketch the meniscus in figure SI3, where we highlight the coexistence of dynamic and static parts drawn with solid and dashed lines, respectively.

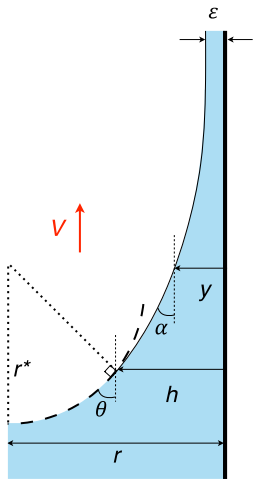

Figure SI3. Sketch of the matching between the static and dynamical part of the meniscus. On the left part of the sketch, the static meniscus is a portion of sphere with radius of curvature r^* while the dynamic meniscus is described in SI1. The matching between the two menisci is done for $y = h$ and $\alpha = \theta$, when the two curvatures balance.

The size h of the dynamical meniscus can be obtained from the matching the curvatures between the part influenced by the flow and the static part of meniscus (with a spherical shape of radius r^*). The curvature induced by the flow in the dynamical part is $2Ca\sin^2(\alpha)/y(\alpha - \cos\alpha \sin\alpha)$ (see SI1) and it is $1/r^* = \cos\theta/(r - h)$ in the static part of the meniscus, which yields:

$$h = 2\,Ca\,(r-h)\frac{\sin\theta\tan\theta}{\theta - \sin\theta\cos\theta} \tag{SI.4}$$

Using eq. (3), we obtain an implicit equation between h and θ for a meniscus advancing on a film of thickness ε in a tube of radius r:

$$h\frac{\ln\frac{h}{\varepsilon}}{r-h} = \frac{\sin\theta\tan\theta}{\theta - \sin\theta\cos\theta}\int_0^{\theta}\frac{\alpha - \sin\alpha\cos\alpha}{2\sin\alpha}\,d\alpha \tag{SI.5}$$

Combined with eq. SI4, we obtain a relation between the angle θ and the thickness of the dynamical meniscus h with the velocity of the meniscus (figure SI4).

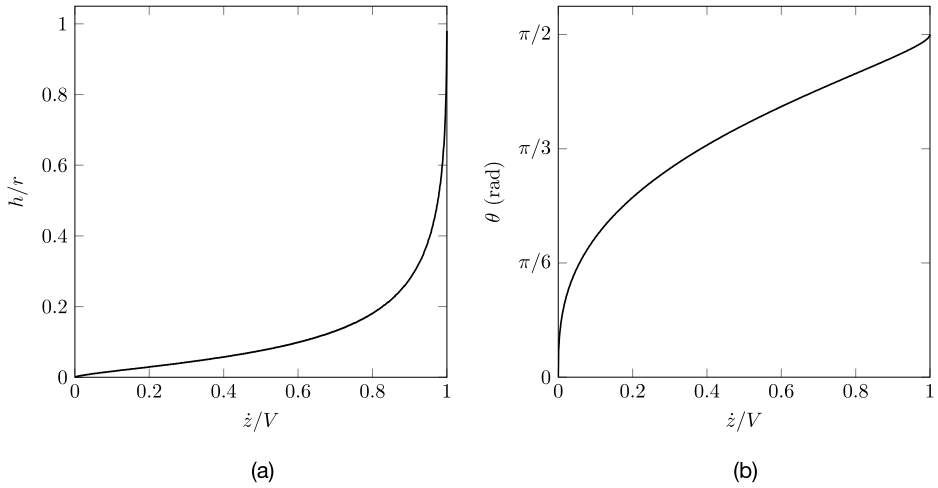

Figure SI4. (a) Thickness of the dynamical meniscus divided by the tube radius and (b) macroscopic contact angle as a function of the meniscus velocity *v* divided by the initial velocity *V* obtained from eq. (4) for a meniscus advancing on film of liquid of thickness $\varepsilon = 1$nm.

The size of the dynamical meniscus h approaches r as the meniscus velocity $\dot{z}$ is close to the initial velocity V (defined by eq. 4). As the meniscus slows down, the size h of the dynamical region rapidly becomes small whereas the angle θ is still rather large. For instance in a tube of radius 0.7 mm, when the velocity has decreased by a factor 2, the thickness of the dynamic meniscus is $h \approx 100$ µm and the contact angle θ is above $\pi/3$ a consequence is that θ appears as a macroscopic contact angle, that depends on the meniscus velocity. We recover in figure SI5.a the shape of the dynamic meniscus with eq. 3 ($y < h(\dot{z})$, solid line), and the static part of curvature $r^* = [r - h(\dot{z})]/\cos\theta(\dot{z})$ ($y > h(\dot{z})$, dashed line).

We can also retrieve the global behavior of the rising liquid column: the meniscus is driven by a force $2\pi\gamma r\cos\theta(\dot{z})$ and slowed down by viscous friction in the bulk ($8\pi\eta z\dot{z}$) and gravity ($\pi r^2\rho gz$) which yields the differential equation SI.6:

$$2r\gamma\cos\theta(\dot{z}) = 8\eta z\dot{z} + r^2\rho gz \qquad \text{(SI.6)}$$

We integrate equation SI.6 to recover the evolution of the meniscus height and compare the numerical integration to the data in figures SI5.b and SI5.c.

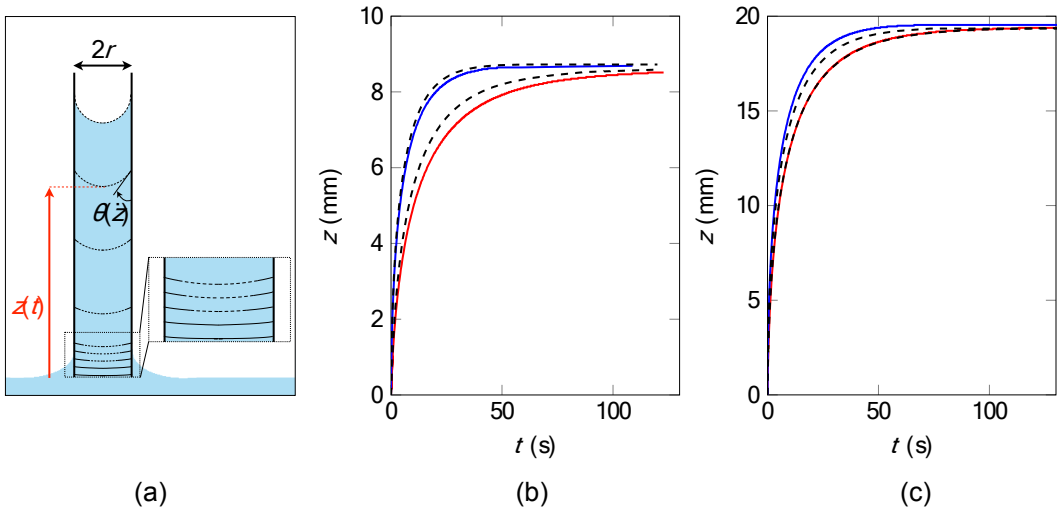

Figure SI5. (a) Meniscus shape at different steps of the rise of a viscous oil (η = 350 mPa.s) in a dry tube (ε = 1 nm) with radius r = 0.7 mm (from bottom to top, t = 0, 0.1, 0.2, 0.3, 0.4, 1.2, 3.5, 9.5, 75.5, 150 s, corresponding to a ratio $\dot{z}/V$ = 1, 0.96, 0.89, 0.76, 0.51, 0.24, 0.09, 0). The solid and dashed lines respectively represent the meniscus part influenced by line friction and the static region (portion of a sphere). In **(b)** and **(c),** we compare the data from figures 1.b and 1.c (coloured lines) and the corresponding numerical integration (dashed black lines) of equation SI.6. **(b)** Silicone oil of viscosity η = 350 mPa.s rising in capillary tube of radius r = 0.5 mm either dry (ε = 1 nm) or prewet (ε = 24 µm). **(c)** Silicone oil of viscosity η = 50 mPa.s rising in capillary tube of radius r = 0.23 mm either dry (ε = 1 nm) or prewet (ε = 4 µm).

As seen in the figure SI5, the numerical integration (black dashed lines) gives accurate results for both dry (blue) and prewet (red) tubes, without any adjustable parameter. The small difference obtained between the numerical and experimental results could reflect small imperfections of the preweting or precursor film thickness.